DNA Structure

DOI: 10.1002/ange.201209144

Effective Chiral Discrimination of Tetravalent Polyamines on the Compaction of Single DNA Molecules**

Yuko Yoshikawa, Naoki Umezawa,* Yuki Imamura, Toshio Kanbe, Nobuki Kato, Kenichi Yoshikawa, Tadayuki Imanaka, and Tsunehiko Higuchi**

Numerous in vitro studies have shown that the binding of natural and synthetic polyamines to DNA induces the condensation/compaction of DNA.[1–6] This phenomenon is of interest in biology and chemistry, since genomic DNA is often found in different degrees of condensation and requires polyamines for the adoption and stabilization of its compact structures.[1,7] Among naturally occurring polyamines, spermine (4+) is much more potent at promoting DNA compaction than putrescine (2+) and spermidine (3+); this observation indicates that the valence strongly influences DNA compaction.[4] Several systematic studies on tetravalent polyamines have shown that their influence on DNA compaction is dependent on the geometrical arrangement of positively charged amino groups.[6,8,9] As well as such geometric effects, chiral effects on DNA compaction have also been reported. Nayvelt et al. studied the influence of the chirality of stereoisomers of α-methylated spermine analogues on DNA condensation by light-scattering experiments, and showed that there is a small but definite difference in the threshold concentration required for DNA condensation; the maximum difference was approximately 20%.[10]

Herein, we describe a method for the highly sensitive chiral discrimination of newly synthesized stereoisomers of tetravalent (4+) polyamines on the basis of their ability to induce compaction in a single molecule of DNA. The polyamines we used are shown in Scheme 1. Since many polyamine receptor sites, such as DNA, are chiral, we envisioned that the introduction of stereogenic centers into a polyamine backbone would affect the activity of the polyamine. The simple incorporation of *trans*-cyclopentane rings into the spermine backbone provided chirality and substantial rigidity. Furthermore, a *p*-methoxyphenyl group was introduced as a chromophore for the detection of UV absorption during HPLC purification and the convenient determination of concentration. These polyamines were synthesized by a method similar to a previously reported procedure (see the Supporting Information).[11–13] Each spermine analogue contained two *trans*-cyclopentane units with a total of four stereogenic centers (Scheme 1).

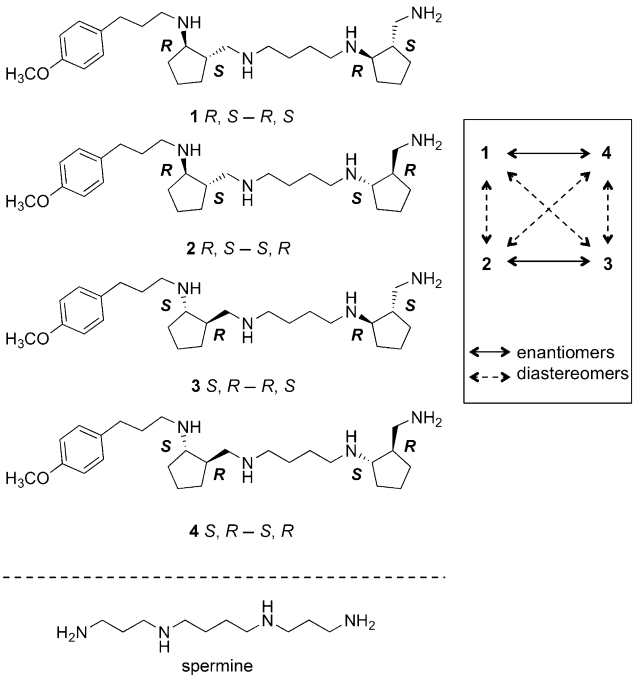

Scheme 1. Chemical structures of spermine and spermine analogues **1**, **2**, **3**, and **4**.

To monitor the changes in the higher-order structure of DNA at the single-molecule level, we used a large genomic DNA molecule, T4 GT7 phage DNA (166 kbp, 57 μm). It has been established that such large DNA molecules undergo a discrete conformational transition from an expanded coil state to a compact state upon the addition of various condensing agents.[4,14,15] We observed the large DNA in the presence and absence of chiral polyamines by fluorescence microscopy. As DNA is a long, thin molecule and shows significant intramolecular and translational Brownian motions in bulk solution, we adapted an inverted wide-field fluorescence microscope for the observations with a relatively

[*] Prof. Dr. Y. Yoshikawa, Prof. Dr. T. Imanaka
Department of Biotechnology, College of Life Sciences
Ritsumeikan University, Kusatsu 525-8577 (Japan)
E-mail: yyoshi@fc.ritsumei.ac.jp
Dr. N. Umezawa, Y. Imamura, Dr. N. Kato, Prof. Dr. T. Higuchi
Graduate School of Pharmaceutical Sciences
Nagoya City University, Nagoya 467-8603 (Japan)
E-mail: umezawa@phar.nagoya-cu.ac.jp
higuchi@phar.nagoya-cu.ac.jp
Prof. Dr. T. Kanbe
Laboratory of Medical Mycology, School of Medicine
Nagoya University, Nagoya 464-0064 (Japan)
Prof. Dr. K. Yoshikawa
Faculty of Life and Medical Sciences
Doshisha University, Kyotanabe 610-0394 (Japan)

[**] This research was supported in part by Grants-in-Aid for Scientific Research from the Japan Science and Technology Agency CREST program, and from the Japan Society for the Promotion of Science (20249006, 22510123, 23240044, 23659058, and 24590142).

Supporting information for this article is available on the WWW under http://dx.doi.org/10.1002/anie.201209144.

high time resolution, that is, 30 frames per second, which is not possible with a confocal microscope. Representative fluorescence images of individual DNA molecules in aqueous solution and the corresponding quasi-3D profiles of fluorescence intensity are shown in Figure 1 a,b. As shown in Figure 1 a, individual DNA molecules existed in a coil conformation in the buffer solution. Upon the addition of **1** to the solution of the DNA, individual DNA molecules underwent a structural transition from a coil state to a compact-globule state via a partial-globule state, in which swollen and shrunken parts coexist in a single DNA molecule. Figure 1 c shows the distribution of the long-axis length of the DNA. It is clear that **1** causes the folding transition from a coil to a compact state in a dose-dependent manner.

Figure 2 shows a comparison of the size distribution of the DNA after the addition of each of the four stereoisomers at different concentrations; the histogram in the top left corner corresponds to the highest concentration of **1** in Figure 1 c. The results clearly indicate that **1** (*R*,*S*–*R*,*S*) is more efficient at promoting DNA compaction than the other stereoisomers. For example, all of the DNA molecules adopt a fully compact state with **1** (*R*,*S*–*R*,*S*) at a concentration of 5 μM. In contrast, essentially no compact DNA molecules exist in the presence of the other three stereoisomers at this concentration: **2**, **3**, and **4** require concentrations higher than 20 μM to induce all of the DNA molecules to adopt a compact state. These results imply that the concentration of **1** required to induce DNA compaction is about 4 times less than that required for the three other stereoisomers. In related studies on the effect of di- and tetraammonium cations with two stereogenic centers on the higher-order structure of T4 DNA molecules, divalent stereoisomers showed a distinct difference in their potency for inducing DNA compaction, whereas there was essentially no difference for tetravalent stereoisomers.[16,17] A theoretical study on chiral discrimination effects upon DNA compaction induced by the above-mentioned ammonium cations suggested that chiral sensitivity can be detected more readily in the case of divalent cations than for tetravalent cations because the latter are all highly potent at inducing DNA compaction.[18] In contrast, the present results clearly show that there is a definite difference in the abilities of tetravalent chiral polyamines with four stereogenic centers to promote DNA compaction.

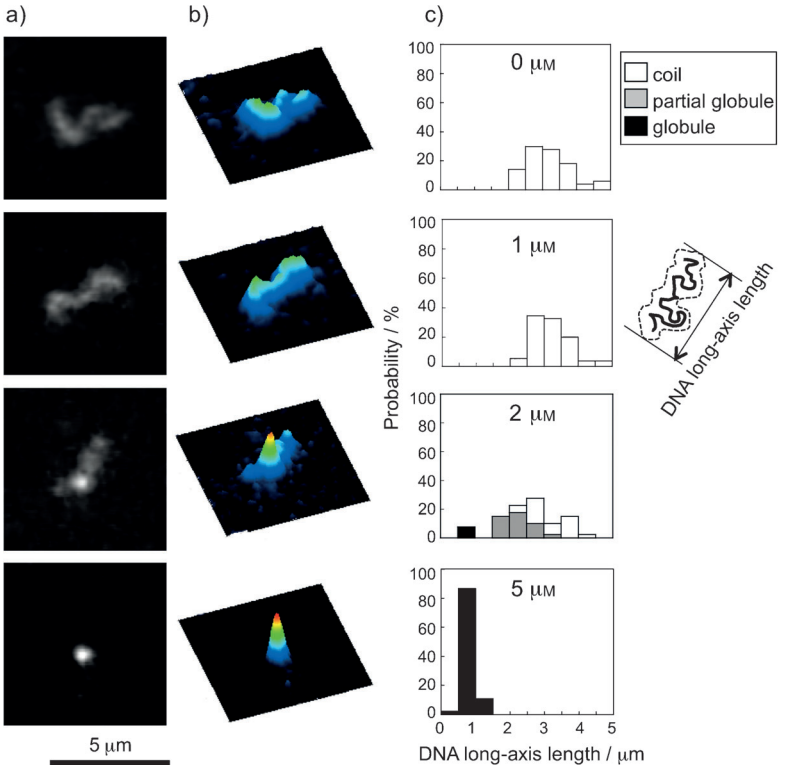

Figure 1. Change in the higher-order structure of T4 DNA in the presence of **1** (0–5 μM). a,b) Fluorescence microscopy images of individual DNA molecules, which exhibit intramolecular and translational Brownian motions in bulk solution, and the corresponding quasi-3D profiles of the fluorescence intensity. c) Distribution of the long-axis length of the DNA and assignment of the conformational characteristics observed in the DNA images: coil, partial-globule, and compact-globule states of single DNA molecules. The DNA concentration was 0.1 μM in nucleotide units. The illustration shows a schematic representation of a fluorescent image of the DNA. Each image was captured at a rate of 30 frames per second.

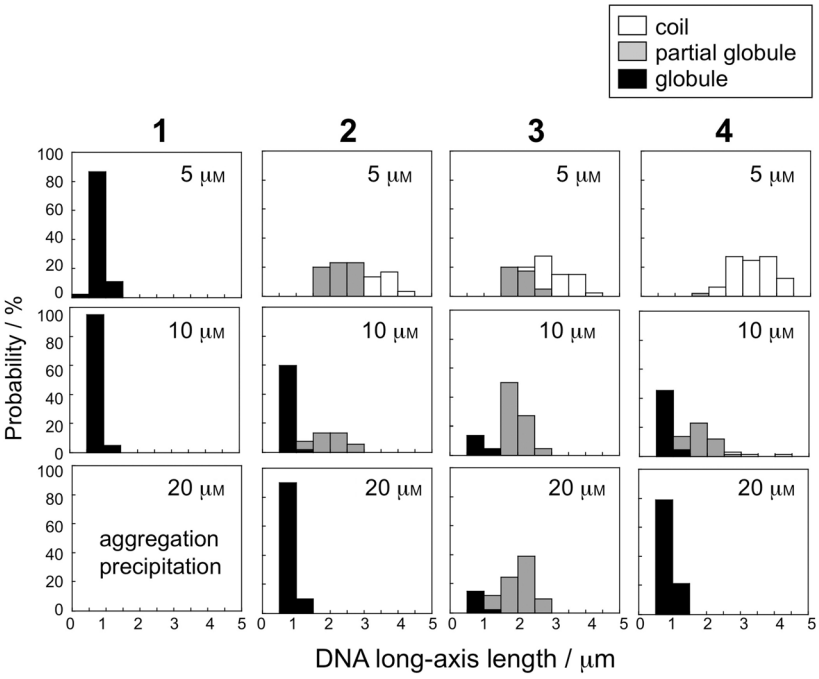

Figure 2. Distribution of the long-axis length of the DNA in solution at various concentrations of **1**, **2**, **3**, and **4**.

We used circular dichroism (CD) spectroscopy to further interpret the effects of chirality on the conformation of DNA. Herein, we do not show CD spectra of long T4 DNA: T4 DNA tended to precipitate at the DNA concentration detectable by CD. Since polyamines were found to bind preferentially to GC-rich DNA,[19,20] we recorded and analyzed CD spectra of poly(dG-dC)·poly(dG-dC) (ca. 1 kbp) in the presence and absence of the four stereoisomers or spermine (Figure 3). A positive Cotton effect at around 280 nm in the CD spectrum corresponds to base stacking, and a negative Cotton effect at around 250 nm corresponds to

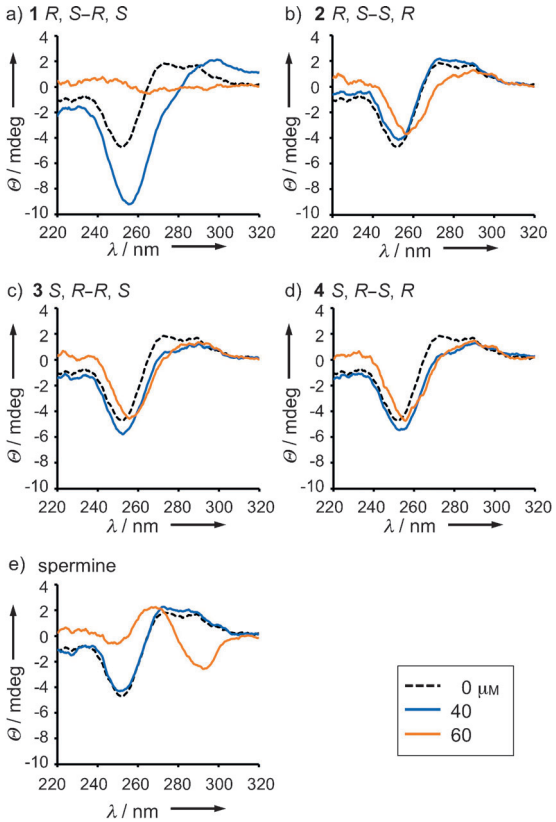

Figure 3. CD spectra of poly(dG-dC)·poly(dG-dC) DNA at various concentrations of **1**, **2**, **3**, **4**, and spermine. The DNA concentration was 50 μM. The polyamine/nucleotide molar ratios were 0, 0.8, and 1.2.

helicity.[21] Upon the addition of **1** (40 μM) to a solution of poly(dG-dC)·poly(dG-dC), the intensity of a band corresponding to a negative Cotton effect increased significantly, which indicates a change in helicity (Figure 3a). For **1** at 60 μM, there was no detectable signal in the CD spectrum, and precipitation was observed (Figure 3a). For **2**, **3**, and **4**, relatively small changes in the CD spectrum were observed at both 40 and 60 μM (Figure 3b,c,d), which indicates that **1** has more influence on the secondary structure. In contrast, spermine induced a B-to-Z transition in the secondary structure of poly(dG-dC)·poly(dG-dC) DNA, as characterized by both a positive signal at 265 nm and a negative signal at 295 nm (Figure 3e). These results suggest that the chiral polyamines interact with DNA in a different manner to spermine.

To evaluate the binding affinity of these chiral isomers for DNA, we performed ^{1}H NMR titration experiments. Poly(dG-dC)·poly(dG-dC) was again used to avoid precipitation: T4 DNA was prone to precipitation under the conditions for NMR titration. Figure 4 shows the ^{1}H NMR signals of the polyamines at around $\delta = 2.3$–2.4 and 2.7 ppm in the presence of poly(dG-dC)·poly(dG-dC) at different concentrations. The signals at $\delta = 2.3$–2.4 and 2.7 ppm were assigned to the hydrogen atoms of the cyclopentane rings and the benzyl hydrogen atoms next to the chromophore, respectively. We did not observe DNA signals in the ^{1}H NMR spectra of the

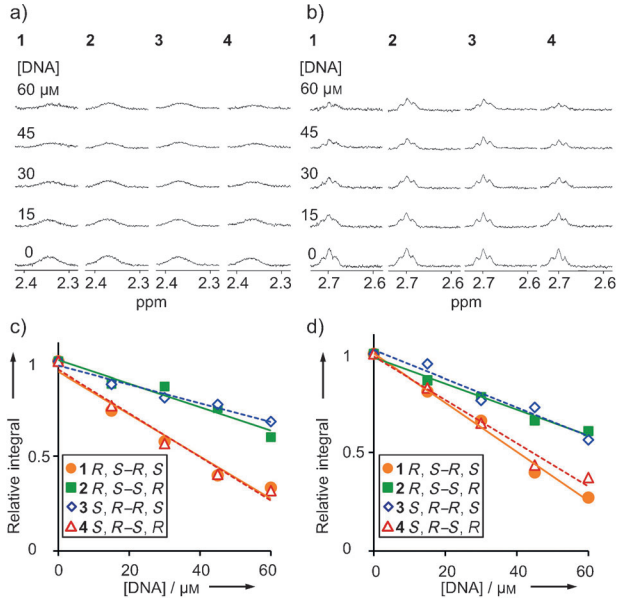

Figure 4. Titration of chiral polyamines (100 μM) with poly(dG-dC)·poly(dG-dC) DNA. ^{1}H NMR spectra in D_2O: a) at $\delta = 2.3$–2.4 ppm, b) at $\delta = 2.6$–2.7 ppm. Decrease upon titration with poly(dG-dC)·poly(dG-dC) DNA in the relative integral of the ^{1}H NMR signal: c) at $\delta = 2.3$–2.4 ppm, d) at $\delta = 2.7$ ppm.

mixtures of the polyamines and DNA. The intensity of the ^{1}H NMR signals observed for the chiral polyamines decreased as the DNA concentration increased, whereas the widths of the signals remained essentially constant. This trend indicates that the bound fraction of the chiral polyamines is not visible in the ^{1}H NMR spectrum, and that the line width, T_2, remains essentially constant for unbound polyamines. Thus, we can evaluate the fraction of unbound chiral polyamines from the change in signal intensity (Figure 4a,b). The difference in the slopes of the regression lines in Figure 4c,d provides information on the binding affinity of the chiral polyamines for DNA. The results show that **1** and **4** exhibit preferential binding to DNA. The binding of **1** and **4** to DNA is about twice as strong as that observed for the other pair of enantiomers, **2** and **3**. This stronger binding by a factor of 2 implies that the difference in the binding free energy, ΔG, is given by Equation (1):

$$\Delta G = R\,T\ln 2 \cong 1.7\ \mathrm{kJ\,mol^{-1}} \qquad (1)$$

in which R is the gas constant ($R = 8.314\ \mathrm{J\,K^{-1}\,mol^{-1}}$) and T is the absolute temperature ($T = 293$ K).

As we demonstrated through a single-molecule observation, isomer **1** (*R*,*S*–*R*,*S*) is more potent at inducing DNA compaction than the other isomers: the threshold concentration of **1** is one quarter of that found for the other isomers (Figure 2). A similar tendency was observed for the efficacy at inducing changes in the secondary structure of DNA, namely, **1** is more effective than the other polyamines (Figure 3). On the other hand, however, ^{1}H NMR titrations showed that the binding potential of the pair of enantiomers **1** and **4** was twice as high as that of the other pair of enantiomers **2** and **3** (Figure 4). These findings clearly indicate that the ability to induce DNA compaction cannot be explained by simple electrostatic binding models. The distinct difference between enantiomers **1** and **4** in their potency for inducing DNA compaction may be directly related to the change in the bending rigidity of double-stranded DNA.

On the basis of the difference in the threshold concentrations of **1** ($c_{R,S-R,S}$) and the other isomers (c_{others}) for the induction of DNA compaction, the difference in the chemical potential, $\Delta\mu$, of these isomers can be expressed by Equation (2):

$$\Delta\mu = -RT(\ln c_{R,S-R,S} - \ln c_{\mathrm{others}}) \cong 3.4\ \mathrm{kJ\,mol^{-1}} \quad (2)$$

On the other hand, the difference in binding free energy between the two pairs of enantiomers (**1** and **4** versus **2** and **3**) is 1.7 kJ mol^{-1}, as calculated from Equation (1). Thus, it becomes apparent that the energy difference for the induction of DNA compaction (3.4 kJ mol^{-1}) is twice as large as that found for the simple electrostatic interaction (1.7 kJ mol^{-1}). By considering these results together with the difference between **1** and **4**, we can conclude that "induced-fit" chiral recognition, rather than an electrostatic interaction, primarily contributes to the difference in the ability to induce DNA compaction.

To gain further insight into the influence of chirality on DNA compaction, we examined compact DNA molecules by transmission electron microscopy (TEM). Figure 5 shows examples of TEM images of T4 DNA compacted by **1** (Figure 5a), its enantiomer **4** (Figure 5b), and spermine (Figure 5c). Assemblies of multiple minitoroidal structures (20 nm in diameter) were observed for DNA compacted by both **1** and **4** (Figure 5a,b). A similar morphology was also observed in the presence of **2** and **3** (see the Supporting Information). There is no apparent difference in the morphology of these structures, even though the threshold concentrations required for DNA compaction are different. In contrast, typical toroids (60–100 nm in diameter)[1–3,22] were observed for spermine-bound compact DNA (Figure 5c). Thus, the chiral tetravalent polyamines caused significant changes in the toroid size and overall morphology of compact DNA.

Interestingly, Shen et al. reported the similar formation of minitoroids when they inserted multiple A-tract sequences into DNA polymers; in this case, DNA compaction was induced by hexamine cobalt(III).[23] An A-tract is a segment that is formed by a number of consecutive adenine residues in a double-helix DNA molecule, and the incorporation of a single A-tract produces a bend as large as 20° in the helical axis of DNA.[23–25] They suggested that curved DNA inserts not only resulted in the generation of a much smaller toroid, but also limited the length of DNA segments contained in each toroid.[23] Our results demonstrate that chiral polyamines promote both the generation of many nucleation centers and the formation of minitoroid clusters in the compaction of DNA without any A-tract inserts (Figure 5). Therefore, we can expect that the binding of chiral isomers to DNA induces substantial bending rigidity and produces an effect similar to the insertion of curved DNA.

We also evaluated the hydrodynamic radius, R_{H}, of the compact DNA through quantitative analysis of the Brownian motion by fluorescence microscopy (see the Supporting Information). It was found that the R_{H} value with **1** was 111 ± 45 nm, whereas the R_{H} value with spermine was 53 ± 16 nm. This result corresponds well with the TEM observations (Figure 5).

In summary, we have synthesized novel stereoisomers of tetravalent (4+) polyamines and examined their ability to induce the compaction of single DNA molecules. Isomer **1** (*R*,*S*–*R*,*S*) is more potent at inducing both DNA compaction and changes in the secondary structure. These results suggest that a cooperative transition of the secondary and higher-order structures of single DNA molecules was induced by chiral polyamines. Minsky suggested previously that the secondary conformation may affect the higher-order structure of DNA.[26] Furthermore, TEM investigations of the compact DNA revealed that chiral polyamines induced the formation of unique assemblies of multiple minitoroidal structures. Since all genomic DNA molecules in living cells are very large, structural transitions in the higher-order structure are believed to play a key role in the mechanism of the self-regulation of genetic activity.[15] The present results highlight the importance of studies on the chiral effect of small ligands on the higher-order structure of giant DNA molecules.

Received: November 15, 2012
Revised: January 26, 2013
Published online: February 25, 2013

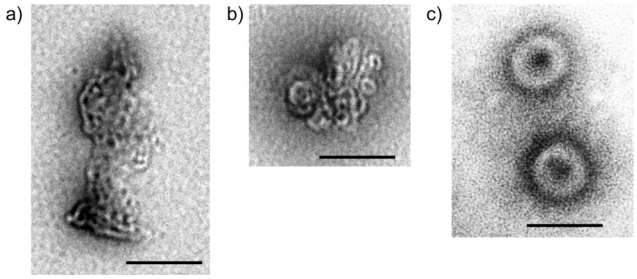

Figure 5. TEM images of compacted T4 DNA in the presence of a) **1** (5 μM), b) **4** (20 μM), and c) spermine (5 μM). Scale bar: 100 nm. The DNA concentration was 0.1 μM.

Keywords: amines · chirality · DNA structures · fluorescence microscopy · single-molecule studies

[1] L. C. Gosule, J. A. Schellman, *Nature* **1976**, *259*, 333 – 335.
[2] D. K. Chattoraj, L. C. Gosule, J. A. Schellman, *J. Mol. Biol.* **1978**, *121*, 327 – 337.
[3] I. Baeza, P. Gariglio, L. M. Rangel, P. Chavez, L. Cervantes, C. Arguello, C. Wong, C. Montanez, *Biochemistry* **1987**, *26*, 6387 – 6392.
[4] M. Takahashi, K. Yoshikawa, V. V. Vasilevskaya, A. R. Khokhlov, *J. Phys. Chem. B* **1997**, *101*, 9396 – 9401.
[5] Y. Yoshikawa, K. Yoshikawa, T. Kanbe, *Langmuir* **1999**, *15*, 4085 – 4088.
[6] M. Saminathan, T. Thomas, A. Shirahata, C. K. Pillai, T. J. Thomas, *Nucleic Acids Res.* **2002**, *30*, 3722 – 3731.
[7] V. A. Bloomfield, *Biopolymers* **1991**, *31*, 1471 – 1481.
[8] H. S. Basu, H. C. A. Schwietert, B. G. Feuerstein, L. J. Marton, *Biochem. J.* **1990**, *269*, 329 – 334.
[9] V. Vijayanathan, T. Thomas, A. Shirahata, T. J. Thomas, *Biochemistry* **2001**, *40*, 13644 – 13651.
[10] I. Nayvelt, M. T. Hyvonen, L. Alhonen, I. Pandya, T. Thomas, A. R. Khomutov, J. Vepsalainen, R. Patel, T. A. Keinanen, T. J. Thomas, *Biomacromolecules* **2010**, *11*, 97 – 105.
[11] J. M. Ostresh, C. C. Schoner, V. T. Hamashin, A. Nefzi, J. P. Meyer, R. A. Houghten, *J. Org. Chem.* **1998**, *63*, 8622 – 8623.
[12] S. Manku, C. Laplante, D. Kopac, T. Chan, D. G. Hall, *J. Org. Chem.* **2001**, *66*, 874 – 885.
[13] C. A. Olsen, M. Witt, J. W. Jaroszewski, H. Franzyk, *J. Org. Chem.* **2004**, *69*, 6149 – 6152.
[14] K. Yoshikawa, Y. Yoshikawa in *Pharmaceutical Perspectives of Nucleic Acid-Based Therapy* (Eds.: R. I. Mahato, S. W. Kim), Taylor and Francis, London, **2002**, pp. 136 – 163.
[15] V. B. Teif, K. Bohinc, *Prog. Biophys. Mol. Biol.* **2011**, *105*, 208 – 222.
[16] A. A. Zinchenko, V. G. Sergeyev, V. A. Kabanov, S. Murata, K. Yoshikawa, *Angew. Chem.* **2004**, *116*, 2432 – 2435; *Angew. Chem. Int. Ed.* **2004**, *43*, 2378 – 2381.
[17] A. A. Zinchenko, C. A. Ning, S. Murata, K. Yoshikawa, *ChemBioChem* **2005**, *6*, 1419 – 1422.
[18] I. A. Nyrkova, A. N. Semenov, *Soft Matter* **2009**, *5*, 979.
[19] K. Igarashi, K. Kashiwagi, *Biochem. Biophys. Res. Commun.* **2000**, *271*, 559 – 564.
[20] K. Higashi, K. Kashiwagi, S. Taniguchi, Y. Terui, K. Yamamoto, A. Ishihama, K. Igarashi, *J. Biol. Chem.* **2006**, *281*, 9527 – 9537.
[21] V. I. Ivanov, L. E. Minchenkova, A. Schyolkina, K. A. I. Poletayev, *Biopolymers* **1973**, *12*, 89 – 110.
[22] N. V. Hud, I. D. Vilfan, *Annu. Rev. Biophys. Biomol. Struct.* **2005**, *34*, 295 – 318.
[23] M. R. Shen, K. H. Downing, R. Balhorn, N. V. Hud, *J. Am. Chem. Soc.* **2000**, *122*, 4833 – 4834.
[24] D. Strahs, T. Schlick, *J. Mol. Biol.* **2000**, *301*, 643 – 663.
[25] C. C. Conwell, I. D. Vilfan, N. V. Hud, *Proc. Natl. Acad. Sci. USA* **2003**, *100*, 9296 – 9301.
[26] A. Minsky, *Annu. Rev. Biophys. Biomol. Struct.* **2004**, *33*, 317 – 342.

